Negative blood oxygenation level dependent homunculus and somatotopic information in primary motor cortex and supplementary motor area

Noa Zeharia[a,b,c], Uri Hertz[a,b,c], Tamar Flash[d], and Amir Amedi[a,b,c,1]

[a]Department of Medical Neurobiology, Institute for Medical Research Israel–Canada, Faculty of Medicine, [b]Interdisciplinary Center for Neural Computation, [c]Cognitive Sciences and The Edmond and Lily Safra Center for Brain Sciences (ELSC), Hebrew University, Jerusalem 91220, Israel; [d]Weizmann Institute of Science, The Department of Computer Science and Applied Mathematics, The Faculty of Mathematics and Computer Science, Rehovot 76100, Israel

Edited* by Emilio Bizzi, Massachusetts Institute of Technology, Cambridge, MA, and approved August 29, 2012 (received for review December 4, 2011)

A crucial attribute in movement encoding is an adequate balance between suppression of unwanted muscles and activation of required ones. We studied movement encoding across the primary motor cortex (M1) and supplementary motor area (SMA) by inspecting the positive and negative blood oxygenation level-dependent (BOLD) signals in these regions. Using periodic and event-related experiments incorporating the bilateral/axial movements of 20 body parts, we report detailed mototopic imaging maps in M1 and SMA. These maps were obtained using phase-locked analysis. In addition to the positive BOLD, significant negative BOLD was detected in M1 but not in the SMA. The negative BOLD spatial pattern was neither located at the ipsilateral somatotopic location nor randomly distributed. Rather, it was organized somatotopically across the entire homunculus and inversely to the positive BOLD, creating a negative BOLD homunculus. The neuronal source of negative BOLD is unclear. M1 provides a unique system to test whether the origin of negative BOLD is neuronal, because different arteries supply blood to different regions in the homunculus, ruling out blood-stealing explanations. Finally, multivoxel pattern analysis showed that positive BOLD in M1 and SMA and negative BOLD in M1 contain somatotopic information, enabling prediction of the moving body part from inside and outside its somatotopic location. We suggest that the neuronal processes underlying negative BOLD participate in somatotopic encoding in M1 but not in the SMA. This dissociation may emerge because of differences in the activity of these motor areas associated with movement suppression.

somatotopy | neural inhibition

One of the most important attributes encoded in motor homunculi is somatotopy. The work by Penfield and Boldrey (1) discovered the ventral-to-dorsal, face-to-leg somatotopic representation in the primary motor cortex (M1) in humans. Subsequent imaging studies have used up to 10 body parts to confirm this organization (2, 3). In the supplementary motor area (SMA), imaging techniques, electrophysiological measurements, and tumor resection have revealed a rostrocaudal, face-to-leg representation in humans (4–6), similar to the representation in primates (7). Studies in the SMA have only used a few body parts and thus, have been unable to show full-body somatotopy.

Our first objective was to map the body representation in M1 and SMA in much greater detail using 20 body parts covering the entire body. Detailed maps on the single-subject level are important for medical purposes as well as assessment of intersubject variability and experience-related plastic changes. We used a continuous cyclic design, enabling us to apply phased-locked analysis approaches, which provide the optimal tools for mapping topographic gradients in the brain (8–11). Our study applies these methods to somatotopic mapping of the motor system.

However, movement encoding does not depend solely on the correct activation of specific muscles but also on the suppression of unwanted ones. The importance of suppressing noninvolved muscles is obvious in motor disorders where the excitation–inhibition balance is disrupted (12). The symptoms of such disorders suggest that, although the excitation–inhibition relationship is often local, it may also be coordinated across the body (e.g., generalized dystonia) (13). Concurrent movements of several limbs in infants also support this view (14). The neuronal control underlying such whole-body coordination is still elusive (15, 16). Thus, we aimed to study the neural correlates of specific body part activation and suppression during movement across M1 and the SMA. Are there coordinated excitatory and inhibitory responses across the entire motor homunculus during single body part movement? What constitutes the spatial organization of these responses? Does inhibition contribute to movement encoding?

We addressed these issues using functional MRI. In general, movement production is accompanied by an increase in firing rate relative to the activity found at rest (1, 6, 7, 17). Numerous functional MRI studies show that movements are also accompanied by an increase in the blood oxygenation level-dependent (BOLD) signal relative to the rest baseline (2), termed positive BOLD. In contrast, negative BOLD is defined as a decrease in the BOLD signal relative to rest (18). Combined BOLD and electrophysiological measurements in the primate visual system (18, 19) have shown that it is associated with a decrease in the neural response. Specifically in the motor system, negative BOLD was found in the ipsilateral hand area in M1 during unimanual hand movements (20, 21), and it was also shown to be related to neural inhibition (22). It is thought to be specifically related to movement suppression of unwanted mirror movements of the contralateral hand (23–25). We, therefore, address the issues of somatotopic representation and coordinated activation and suppression of muscles during movement as indicated by positive and negative BOLD signals in M1 and the SMA.

Results

Whole-Body Highly Detailed Somatotopy in M1 and the SMA. A full-body somatotopy of 20 body parts in M1 and the SMA was assessed using a slow event-related and periodic experimental design. In both experiments, subjects moved 20 body parts separately. The movements were either synchronized in-phase bilateral movements (e.g., concurrent movements of the toes on the left and right feet) or axially symmetric body part movements (e.g., side-to-side movements of the tongue). Electromyographic (EMG) signals were recorded during the scan in several subjects

Author contributions: N.Z., T.F., and A.A. designed research; N.Z. performed research; N.Z., U.H., T.F., and A.A. contributed new reagents/analytic tools; N.Z., U.H., and A.A. analyzed data; and N.Z., U.H., T.F., and A.A. wrote the paper.

The authors declare no conflict of interest.

*This Direct Submission article had a prearranged editor.

Freely available online through the PNAS open access option.

[1]To whom correspondence should be addressed. E-mail: amira@ekmd.huji.ac.il.

This article contains supporting information online at www.pnas.org/lookup/suppl/doi:10.1073/pnas.1119125109/-/DCSupplemental.

to ensure that the movements were correctly carried out and exclude the possibility of movement of other body parts (Figs. S1 and S2). In each block of the event-related experiment, a single body part was moved by the subjects for 4.5 s followed by 12-s rest. In the periodic design experiment, the 20 body parts were moved consecutively in a fixed order; each body part was moved for 3 s, and the movement cycle, consisting of movements of all 20 body parts, was followed by 12 s rest and repeated eight times in each direction (toes to tongue and tongue to toes).

To characterize the whole-body somatotopy in M1, we first analyzed the slow event-related data using the general linear model (GLM) (2, 3). Fig. 1*A*, *Left* shows the activations of all 20 body parts at the same statistical threshold. Although there was substantial overlap in the representation of nearby body parts, face-, hand-, or leg and trunk-related body parts activated separate regions. Fig. 1*A*, *Right* shows the location of the peak activation in each hemisphere of each body part in M1 vs. all of the others masked by this body part vs. rest (Table S1). The activations followed the ventral-to-dorsal, tongue-to-toes organization as in previous studies (1, 2).

The cyclic design of the periodic experiment allowed for periodic analysis, which is considered optimal for analyzing gradual topographic representations (8). Two periodic analysis methods were used (*Methods*). First, we applied cross-correlation analysis (Fig. 1*B*) (26). A hemodynamic response function (HRF) predictor corresponding to the movement time of a single body part was cross-correlated with the BOLD signal. In each voxel, one shifted predictor, corresponding to one body part, was chosen. Second, we used spectral analysis (Fig. 1*C*); Fourier analysis in the movement repetition frequency obtains a phase value serving as a measure for the body part moved (9, 27–29). Both methods (Fig. 1 *B* and *C*) revealed a detailed, continuous, gradual shift in the somatotopic representation in M1 and the known ventral-to-dorsal, tongue-to-toes organization. The results using both methods were consistent, which was shown by the significant alignment index (10) (Fig. 1*D*).

GLM analysis of the slow event-related experiment also provided detailed whole-body somatotopic mapping in the SMA (Fig. 1*E* and Table S2). The 20 activation peaks created a gradually shifting rostrocaudal tongue-to-toes representation with a large degree of overlap. Spectral analysis also revealed this mapping (Fig. 1*F*).

Coarse Negative BOLD Homunculus in M1. In addition to the positive BOLD, the movements were also associated with negative BOLD in M1. Positive and negative BOLD were observed using GLM analysis, in which the rest periods were modeled implicitly. Because negative BOLD was defined as a decrease in the BOLD signal relative to the rest baseline, it was seen when contrasting movements with rest.

The negative BOLD was assessed using the slow event-related experiment as well as an additional block design experiment in which subjects moved only legs, hands, and tongue in a randomized order (9 s movement and 9 s rest). The results of the latter experiment reveal a somatotopic organization of the negative BOLD in M1 (Fig. 2*A*). Where tongue movements elicited positive BOLD, hands and legs elicited negative BOLD; where hand movements elicited positive BOLD, legs and tongue elicited negative BOLD, and where leg movements elicited positive BOLD, the hands and tongue elicited negative BOLD. These movements elicited only positive BOLD in the SMA (Fig. 2*B*). Importantly, a similar pattern of negative BOLD in M1 also appeared in all subjects in the slow event-related experiment

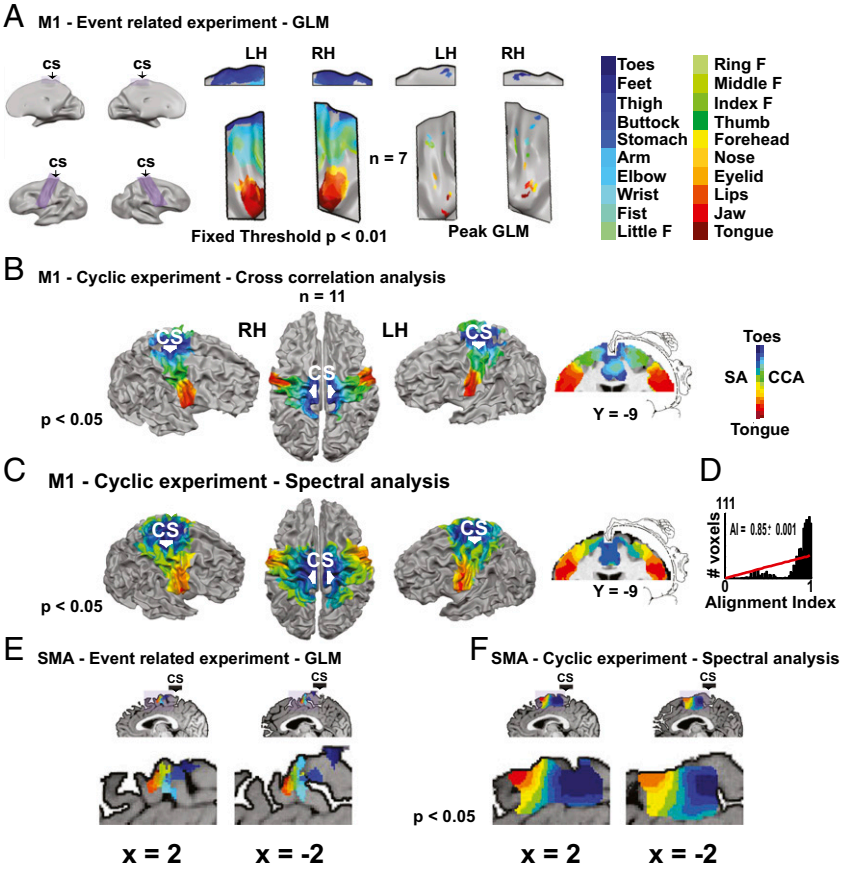

Fig. 1. Twenty body part whole-body somatotopy in M1 and the SMA is shown by GLM and phase-locked analyses (group results; random effect). (*A*) Activations of 20 body parts in the slow event-related experiment in M1 using GLM analysis. The lateral and medial areas of M1 are enlarged (purple). The results are shown at a fixed threshold when contrasting each body part with rest (*Left*) or peak activation when contrasting each body part vs. all of the others masked by contrasting this body part with rest (*Right*). (*B*) Full-body homunculus in M1 obtained by cross-correlation analysis of the periodic experiments. Data are shown on the surface of the brain and a coronal slice, which also shows the original Penfield homunculus. $R > 0.34$. [From Penfield/Rasmussen. *The Cerebral Cortex of Man: A Clinical Study of Localization of Function*. ©1950 Gale, a part of Cengage Learning, Inc. Adapted with permission from (39).] (*C*) The same as in *B* but using spectral analysis. $R > 0.41$. [From Penfield/Rasmussen. *The Cerebral Cortex of Man: A Clinical Study of Localization of Function*. ©1950 Gale, a part of Cengage Learning, Inc. Adapted with permission from (39).] (*D*) Histogram of the similarity index in the voxels in M1. This index quantifies the difference in the phase values obtained using cross-correlation and spectral analysis. The similarity index was highly significant ($P < 0.001$), and the histogram was significantly different from a random distribution (red line), suggesting that these two methods give comparable results. (*E*) Peak activation of all 20 body parts in the SMA in the slow event-related experiment. Each activation was extracted by contrasting each body part vs. the rest. (*F*) Spectral analysis of the periodic experiments in the SMA. $R > 0.41$.

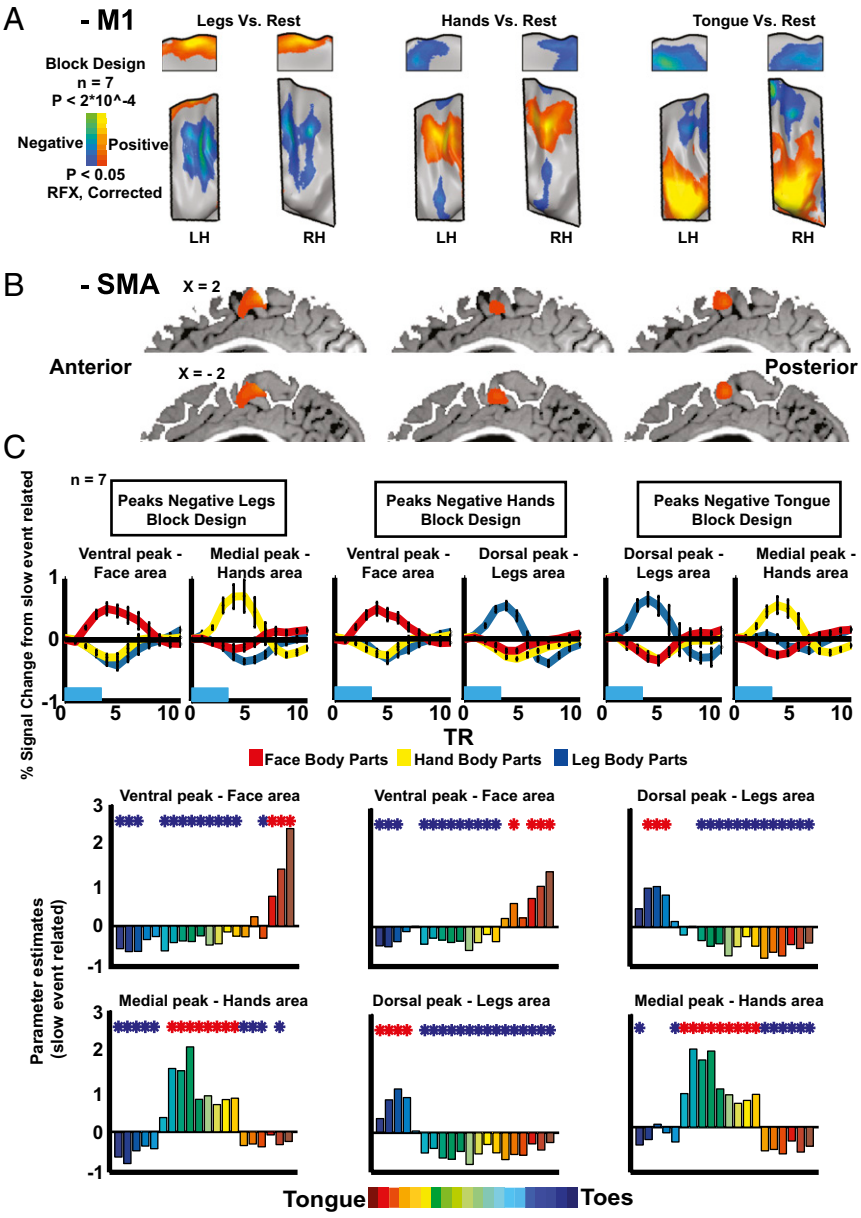

Fig. 2. Negative BOLD in M1 is organized somatotopically, inverse to the positive BOLD. (*A*) Statistical parametric maps of positive and negative BOLD in response to leg (*Left*), hand (*Center*), and tongue (*Right*) movements (random effect; corrected) in the block design experiment. Negative BOLD is somatotopically organized in M1 and adjacent to the positive BOLD. (*B*) Statistical parametric maps in response to leg, hand, and tongue movements (random effect; corrected,) in the block design experiment masked by medial Brodmann area 6. No negative BOLD appears in the SMA. (*C Upper*) ROI analysis of the slow event-related experiment. ROIs were defined by the block design experiment as dorsal and ventral peaks of negative BOLD in M1 in response to leg (*Left*), hand (*Center*), and tongue (*Right*) movements. The average group time course for movements of leg (blue), hand (yellow), and face (red) body parts is shown. (*C Lower*) GLM parameter estimators of the event-related experiment in the same ROIs.

(Fig. S3), showing its consistency at the single-subject level as well.

To further characterize the positive and negative BOLD across M1, a region of interest (ROI) analysis was conducted (Fig. 2*C*). Using the group results from the block design experiment that served as an external localizer, we defined the ROIs as the dorsal and ventral peaks of negative BOLD in M1 for tongue, hand, and leg movements (Fig. 2*C*, *Upper*). In these peaks, we illustrate the group event-related averaging of the time course of the face, hand, and leg body parts from the slow event-related experiment. In each negative BOLD peak, one group of body parts elicited positive BOLD, whereas the other two groups elicited negative BOLD (although the ROIs were defined as the peak negative BOLD of only one body part in the block design experiment), strengthening their inverse spatial patterns. The time courses of the positive and negative BOLD in the same ROI were similar; no significant difference ($P < 0.13$) was found between the times to peak of the negative (8.5 ± 0.1 s) and positive (8 ± 0.2 s) BOLD. However, the maximum amplitude of the negative BOLD ($-0.35 \pm 0.01\%$ signal change) was about 52% of the amplitude of the positive BOLD ($0.67 \pm 0.06\%$), and this difference was significant ($P < 10 \times 10^{-23}$).

To characterize the whole activation tuning curve, group GLM analysis was applied to the same ROIs, and GLM parameter estimator values were extracted for the 20 body parts from the slow event-related experiment (Fig. 2*C*, *Lower*). A significant positive or negative BOLD was observed for most body parts in each ROI. Although nearby body parts showed positive parameter estimators with different magnitudes, distant body parts showed negative ones, supporting the somatotopic organization of the negative BOLD in M1. These results are consistent with the work by Meier et al. (2).

The inverse relations of the positive and negative BOLD in M1 are clearly visible when the statistical parametric maps from Fig. 2*A* are plotted separately for positive or negative BOLD (Fig. 3). Given the clear large-scale somatotopic organization of the negative BOLD, we term it the coarse negative BOLD homunculus. The possible relations between this organization and the coordination of excitation and suppression across the body are discussed below.

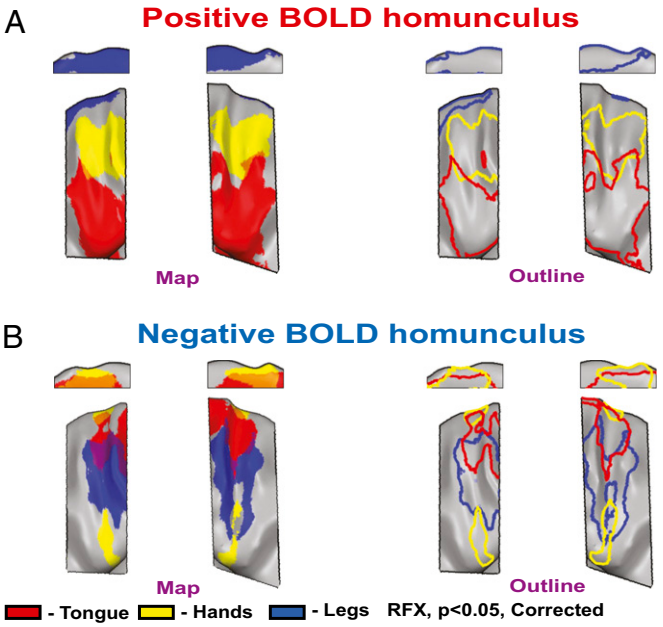

Fig. 3. The coarse negative BOLD homunculus. (*A*) The combined positive BOLD responses to leg, hand, and tongue movements from Fig. 2*A* (*Left*, full map; *Right*, outline; red, tongue; yellow, hands; blue, legs) revealing the known positive homunculus in M1. (*B*) The combined negative BOLD responses to leg, hand, and tongue movements from Fig. 2*A* (*Left*, full map; *Right*, outline; red, tongue; yellow, hands; blue, legs) showing a coarse negative homunculus in M1.

Predictive Somatotopic Information in Positive and Negative BOLD in M1 and the SMA. To characterize the somatotopic information in the positive BOLD in M1 and the SMA and negative BOLD in M1, we used multivoxel pattern analysis (MVPA) to investigate whether they allowed for prediction of the identity of a single moving body part (Fig. 4). Such a prediction is only possible if the BOLD signal contains somatotopic information.

We first defined the data to be classified from the event-related experiment separately for each subject. The 20 body parts were divided into three groups: leg and trunk (toes, feet, thighs, buttocks, and stomach), hand (upper arm, elbow, wrist, fist, and all five fingers), and face (forehead, nose, eyelids, lips, jaw, and tongue) body parts. We then defined the areas for classification in M1 and the SMA. Three ROIs were defined separately for each subject and each body part group: the positive representation of the classified body parts in M1 and the SMA and their negative representation in M1. For each body part group, we trained and tested a multiclass support vector machine on each ROI. Significance was assessed using a random permutation test.

The group average classification results (Fig. 4) show that, by using the positive BOLD ROIs in M1 and the SMA, a significant classification of the moving body part from among a group of close body parts was possible (e.g., using the positive hand ROI in M1 and the SMA, it was possible to predict which body part was moved from among the nine hand body parts). Classification using the positive BOLD in M1 was always higher than classification using the positive BOLD in the SMA, but this trend was significant only for the face and hand body parts ($P < 10 \times 10^{-6}$ and $P < 10 \times 10^{-5}$, respectively).

Importantly, significant classification was also possible using the negative BOLD in M1. However, it was significantly lower than the classification using the positive BOLD ($P < 2.5 \times 10^{-5}$, $P < 2.5 \times 10^{-4}$, and $P < 0.01$ for face, hand, and leg body parts, respectively). Classification using the positive BOLD in the SMA was only significantly higher than the classification using the negative BOLD for the leg ($P < 0.02$) but not for hand ($P < 0.054$) or face ($P < 0.75$) parts. This finding suggests that, although the negative BOLD is located outside the somatotopic location of the classified body parts (e.g., the negative BOLD elicited by hand movements is located in the leg and face areas), it nonetheless contains somatotopic information.

Additional control ROIs were examined to exclude classification resulting from nonneuronal factors (*SI Text*).

Discussion

In this study, we have shown that periodic analysis allows for a detailed, full-body somatotopic mapping in the motor system. Additionally, we show that the negative BOLD signal is organized somatotopically in M1 in an inverse spatial relationship to the positive BOLD. Finally, we show that negative BOLD outside the somatotopic location contains predictive somatotopic information, as well as the positive BOLD in M1 and the SMA.

Periodic Analysis Provides a Fast, Efficient, Noninvasive Method for Obtaining Whole-Body Somatotopic Motor Maps. In this study, we used three methods of somatotopic mapping: GLM, cross-

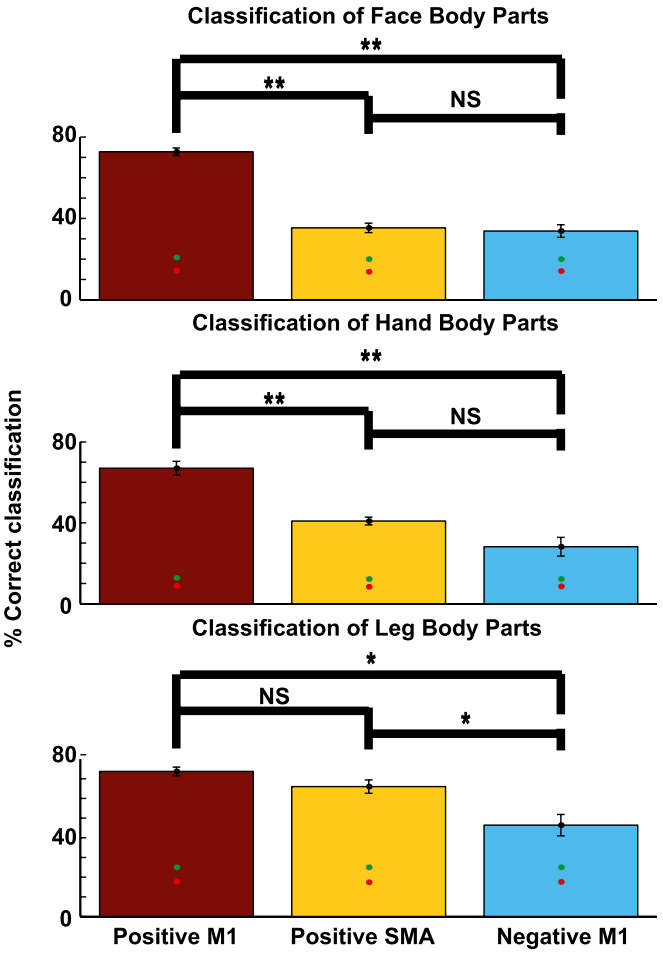

Fig. 4. Predictive somatotopic information in positive BOLD in M1 and the SMA and negative BOLD in M1. Group results of MVPA classification of movement of face (*Top*), hand (*Middle*), and leg and trunk (*Bottom*) body parts from the slow event-related experiment. Each group of body parts was classified in the respective positive BOLD ROIs in M1 (red) and the SMA (orange) and negative BOLD ROIs in M1 (light blue). The ROIs were defined in each subject individually. The identity of the moving body parts can be predicted from positive BOLD in M1 and the SMA but also from negative BOLD in M1, which is located outside the somatotopic area. Red and green dots indicate the mean and 95th percentile of a random shuffled permutation test, respectively. *$P < 0.02$; **$P < 2.5 \times 10^{-4}$.

correlation, and spectral analysis. GLM is the traditional method for analyzing somatotopic gradients in the motor system, and it serves to identify peak activation and contrasts between body parts (2, 3). However, GLM analysis is still limited in mapping gradual shifts of representation (*SI Text* and Fig. S4).

In contrast to somatotopic motor mapping, retinotopic mapping is usually based on phase-locking analytic approaches. These approaches are considered the classical means of defining early visual areas (9, 30) and also used to map other sensory systems (11, 26, 28). They yield a highly robust topographic mapping and can pinpoint gradients undetected by GLM analysis (8). They also require a shorter scanning time and fewer repetitions, which can be crucial in medical settings.

Here, we used two such periodic analysis methods. The cross-correlation method considers the canonical HRF like the GLM method does, but it enables a periodic analysis. This method is a winner takes all method; for each voxel, only one shifted predictor, corresponding to one body part, is chosen. This method provides a clear estimation of the most represented body part. Because predictor duration corresponds to the movement duration of one body part, this analysis is more suitable when the overlap in representation of various body parts is fixed and relatively small.

By contrast, spectral analysis, which does not rely on an HRF model, is less sensitive to the shape of the hemodynamic response and more driven by its periodicity and timing. It can, therefore, identify various activation shapes (which are wider in a continuous design experiment when the overlap in representation increases), including broadly tuned or highly selective voxels.

Although the main results in all of the data analysis techniques were similar (Fig. 1), they also suggest that periodic analysis provides a faster, more efficient noninvasive method for obtaining whole-body somatotopic motor maps, thus confirming and greatly extending available knowledge on somatotopy (2–6). The periodic experimental design can serve as a standard procedure for mapping motor homunculi. The fact that such detailed maps could be obtained quickly at the single-subject level (Figs. S5 and S6) is critical for medical purposes. Additional homunculi were also mapped but are beyond the scope of the current paper.

Somatotopic Organization, Predictive Information, and Possible Underlying Mechanisms of Negative BOLD in M1. Whole-brain and ROI analyses (Figs. 2 and 3) have shown that negative BOLD in M1 is somatotopically organized in an inverse spatial pattern compared with the positive BOLD. This mirror organization, as well as the temporal characteristics of the time courses, resembles the organization of positive and negative BOLD in early visual areas (19).

Classification was possible using the negative BOLD, indicating that it contains somatotopic information, although it is outside the activated somatotopic location. The significant positive or negative influences of various body parts in each ROI across M1 also support a distributed representation of different types of information across M1. Similar stimulus-specific distributed information in the negative BOLD has also been found in the visual (31) and auditory (32) systems.

Reports have argued for a neural origin of the negative BOLD in the visual (18, 19) and motor (22) systems. The large-scale somatotopic organization of negative BOLD across M1 found here provides a unique opportunity for examining the possible sources of negative BOLD adjacent to positive BOLD within the same functional area. The hemodynamic blood-stealing phenomenon (19) cannot account for the negative BOLD here, because the blood to the lateral M1 (hands and face areas) derives from the middle cerebral artery, but the anterior cerebral artery supplies the medial portion of M1 (leg areas) (33).

Additional studies are needed to explain the relations of negative BOLD to movement suppression. Here, subjects were specifically instructed to move only one body part. This may increase inhibition and negative BOLD. Although in natural activity, one usually does not think about not moving other body parts, this form of coordinated movement suppression across the body may still be present (13, 14).

The presence of negative BOLD in M1 but not the SMA may be explained by previous studies showing that movement suppression seems related to SMA activation (34) and both positive and negative BOLD in M1 (22). As to the possible neuronal connections underlying such nonsomatotopic inhibition, because the movements in this study were bilateral, we cannot determine whether the negative BOLD arises from intra- or interhemispheric connections. Evidence exists for both types of nonhomotopic connections in M1 (35) as well as nonsomatotopic inhibition from the contralateral M1 (36). Connections from secondary motor cortices could also induce nonsomatotopic inhibition in M1 during movement (37).

If the negative BOLD found here is, indeed, related to neural inhibition, its somatotopic organization and predictive information might shed light on the mechanisms behind the balance between suppression and activation of muscles across the body.

Methods

Subjects. Sixteen healthy, right-handed subjects (eight women) participated in the periodic (11 subjects), slow event-related (7 subjects), and block design (the same 7 subjects) experiments. The experimental procedure was approved by the local Ethics Committee, and written informed consent was obtained from all subjects.

The movements in all three experimental designs were bilateral or involved an axial body part. Bilateral movements served to map positive BOLD homunculi in both hemispheres as well as negative BOLD during bilateral movements. It was also used given the presumed role of SMA in driving bilateral movements.

Periodic Design Experiments. Subjects moved 20 body parts consecutively according to an auditory cue. Each movement cycle included the movements of all 20 body parts and lasted 60 s. Each cycle was followed by a 12-s rest. There were eight repetitions of the movement cycle in each direction (from toes to tongue and from tongue to toes). Each body part was moved three times at a frequency of 1 Hz. This design enabled the use of phase-locked analysis.

In the two other experiments, the movements of the different body parts were separated by a long rest period, and their order was randomized. These experiments enabled a clean inspection of positive and negative BOLD.

Slow Event-Related Experiment. All 20 body parts in the periodic design experiments were moved 20 times each (4.5 s movement and 12 s rest). Five movements were performed in each event at a frequency of 1 Hz. In five subjects, EMGs were recorded. This design enabled a detailed analysis of positive and negative BOLD signals of each body part and the use of MVPA.
Block design. Tongue, hands, and feet were moved in separate blocks (9 s movement and 9 s rest). Nine movements were performed in each block at a frequency of 1 Hz. The block design experiment was analyzed separately and also served as an external localizer for the ROI analysis.
GLM analysis. All contrasts showing positive or negative BOLD were derived by contrasting the movement period vs. rest baseline (the rest period was modeled implicitly). All random effect results (except for three nonsignificant peaks of activations in Fig. 1*A*) were corrected for multiple comparisons using the Monte Carlo (38) method (1,000 iterations, $\alpha < 0.05$) (Table S1). The a priori threshold for correction in the block design was set to $P < 0.05$ (Figs. 2 *A* and *B* and 3). Higher statistical thresholds were used in the analysis of the event-related design because of the higher number of repetitions (20 repetitions compared with 8 repetitions in the block design). For the group analysis (Fig. 1*A*, *Left*), the a priori threshold was $P < 0.01$. For the single-subject analysis (Fig. S3) the a priori threshold was $P < 0.001$ given the high variability and larger degrees of freedom at this level. The a priori statistical thresholds for the peaks of activation (Fig. 1 *A*, *Right* and *E*) are given in Tables S1 and S2. Three of the peaks were not significant. Fig. S7 presents only the significant peaks.

Spectral Analysis. Fourier analysis was applied to the time course of each voxel and was locked to the movement repetition frequency (*SI Text*). The Fourier

analysis delivered amplitude and phase values that were used to construct a pure cosine at the movement frequency. This construction served as a model of activation. A Pearson correlation coefficient was calculated between this model and the time course as a direct measure of the response to the movement of the voxel. The phase value was inspected in regions showing high correlation to the movement repetition frequency. Phase values were distributed between $-\pi$ and π and represented time points within the movement cycle.

The random effect group results were corrected for multiple comparisons using the Monte Carlo method (1,000 iterations, $\alpha < 0.05$) with an a priori threshold of $P < 0.05$.

Cross-Correlation Analysis. A boxcar function 2 Time of Repetition (TRs) long (the duration of movement of one body part) was convolved with a canonical hemodynamic response function, resulting in the predictor for this analysis. This predictor and the time course of each voxel were cross-correlated, allowing for 40 lags with one TR interval time to account for the movement duration of the movement cycle (40 TRs). For each voxel, we obtained the lag value with the highest correlation coefficient between the time course and 1 of 40 predictors and the value of this correlation coefficient. Because all body parts were moved consecutively, the lag value corresponded to the moved body part (two lags per body part).

The random effect results were corrected for multiple comparisons ($\alpha < 0.05$) using the Monte Carlo method with an a priori threshold of $P < 0.05$.

Map Alignment Measure. An alignment index was calculated voxelwise as (Eq. **1**)

$$Alignment\_Index = 1 - \frac{|\Delta\phi|}{\pi}, \quad [1]$$

where $\Delta\phi$ is the difference between the phases.

MVPA. MVPA was conducted for each subject separately. The ROIs were defined separately for each subject [False Discovery Rate (FDR) corrected, $\alpha < 0.05$]. The uncorrected values ranged between $P < 0.023$ and $P < 0.039$.

SI Text has additional information on experimental protocols, EMG measurements, data processing, and analysis.

ACKNOWLEDGMENTS. We thank Dr. Edna Furman-Haran, Mr. Nachum Stern, and Mrs. Fanny Attar for assistance with the experiments and Prof. Jenny Kien for editorial assistance. T.F. is the incumbent of the Dr. Hymie Moross Professorial chair. This research was funded by the International Human Frontier Science Program Organization (HFSPO) (to A.A.), Israel Science Foundation Grant 1530/08 (to A.A.), European Union Marie Curie International Reintegration Grant MIRG-CT-2007-205357 (to A.A.), James S. McDonnell Foundation Scholar Award 220020284 (to A.A.), European Commission Grants FP7-ICT-2009-C-Tango and FP7-ICT-2009-C-Vere (to T.F.), and the Edmond and Lily Safra Center for Brain Sciences and the Charitable Gatsby Foundation (A.A.).

1. Penfield W, Boldrey E (1937) Somatic motor and sensory representation in the cerebral cortex of man as studied by electrical stimulation. *Brain: A Journal of Neurology* 60:389–443.
2. Meier JD, Aflalo TN, Kastner S, Graziano MSA (2008) Complex organization of human primary motor cortex: A high-resolution fMRI study. *J Neurophysiol* 100:1800–1812.
3. Schieber MH (2001) Constraints on somatotopic organization in the primary motor cortex. *J Neurophysiol* 86:2125–2143.
4. Chainay H, et al. (2004) Foot, face and hand representation in the human supplementary motor area. *Neuroreport* 15:765–769.
5. Chassagnon S, Minotti L, Kremer S, Hoffmann D, Kahane P (2008) Somatosensory, motor, and reaching/grasping responses to direct electrical stimulation of the human cingulate motor areas. *J Neurosurg* 109:593–604.
6. Hanakawa T, et al. (2001) Functional mapping of human medial frontal motor areas. The combined use of functional magnetic resonance imaging and cortical stimulation. *Exp Brain Res* 138:403–409.
7. Luppino G, Matelli M, Camarda RM, Gallese V, Rizzolatti G (1991) Multiple representations of body movements in mesial area 6 and the adjacent cingulate cortex: An intracortical microstimulation study in the macaque monkey. *J Comp Neurol* 311: 463–482.
8. Engel SA (2012) The development and use of phase-encoded functional MRI designs. *Neuroimage* 62:1195–1200.
9. Engel SA, et al. (1994) fMRI of human visual cortex. *Nature* 369:525.
10. Sereno MI, Huang RS (2006) A human parietal face area contains aligned head-centered visual and tactile maps. *Nat Neurosci* 9:1337–1343.
11. Striem-Amit E, Hertz U, Amedi A (2011) Extensive cochleotopic mapping of human auditory cortical fields obtained with phase-encoding FMRI. *PLoS One* 6:e17832.
12. Tinazzi M, et al. (2005) Task-specific impairment of motor cortical excitation and inhibition in patients with writer's cramp. *Neurosci Lett* 378:55–58.
13. Sanger TD, Delgado MR, Gaebler-Spira D, Hallett M, Mink JW Task Force on Childhood Motor Disorders (2003) Classification and definition of disorders causing hypertonia in childhood. *Pediatrics* 111:e89–e97.
14. Thelen E, Kelso J, Fogel A (1987) Self-organizing systems and infant motor development. *Dev Rev* 7:39–65.
15. Brown P, Day BL, Rothwell JC, Thompson PD, Marsden CD (1991) Intrahemispheric and interhemispheric spread of cerebral cortical myoclonic activity and its relevance to epilepsy. *Brain* 114:2333–2351.
16. Huntley GW, Jones EG (1991) Relationship of intrinsic connections to forelimb movement representations in monkey motor cortex: A correlative anatomic and physiological study. *J Neurophysiol* 66:390–413.
17. Woolsey CN, et al. (1952) Patterns of localization in precentral and "supplementary" motor areas and their relation to the concept of a premotor area. *Res Publ Assoc Res Nerv Ment Dis* 30:238–264.
18. Shmuel A, Augath M, Oeltermann A, Logothetis NK (2006) Negative functional MRI response correlates with decreases in neuronal activity in monkey visual area V1. *Nat Neurosci* 9:569–577.
19. Shmuel A, et al. (2002) Sustained negative BOLD, blood flow and oxygen consumption response and its coupling to the positive response in the human brain. *Neuron* 36:1195–1210.
20. Ferbert A, et al. (1992) Interhemispheric inhibition of the human motor cortex. *J Physiol* 453:525–546.
21. Perez MA, Cohen LG (2008) Mechanisms underlying functional changes in the primary motor cortex ipsilateral to an active hand. *J Neurosci* 28:5631–5640.
22. Stefanovic B, Warnking JM, Pike GB (2004) Hemodynamic and metabolic responses to neuronal inhibition. *Neuroimage* 22:771–778.
23. Allison JD, Meador KJ, Loring DW, Figueroa RE, Wright JC (2000) Functional MRI cerebral activation and deactivation during finger movement. *Neurology* 54:135–142.
24. Nass R (1985) Mirror movement asymmetries in congenita1 hemiparesis. *Neurology* 35:1059.
25. Sehm B, Perez MA, Xu B, Hidler J, Cohen LG (2010) Functional neuroanatomy of mirroring during a unimanual force generation task. *Cereb Cortex* 20:34–45.
26. Orlov T, Makin TR, Zohary E (2010) Topographic representation of the human body in the occipitotemporal cortex. *Neuron* 68:586–600.
27. Engel SA, Glover GH, Wandell BA (1997) Retinotopic organization in human visual cortex and the spatial precision of functional MRI. *Cereb Cortex* 7:181–192.
28. Hertz U, Amedi A (2010) Disentangling unisensory and multisensory components in audiovisual integration using a novel multifrequency fMRI spectral analysis. *Neuroimage* 52:617–632.
29. Sereno MI, et al. (1995) Borders of multiple visual areas in humans revealed by functional magnetic resonance imaging. *Science* 268:889–893.
30. Wandell BA, Winawer J (2011) Imaging retinotopic maps in the human brain. *Vision Res* 51:718–737.
31. Bressler D, Spotswood N, Whitney D (2007) Negative BOLD fMRI response in the visual cortex carries precise stimulus-specific information. *PLoS One* 2:e410.
32. Linke AC, Vicente-Grabovetsky A, Cusack R (2011) Stimulus-specific suppression preserves information in auditory short-term memory. *Proc Natl Acad Sci USA* 108: 12961–12966.
33. Kiernan JA (2009) *Barr's the Human Nervous System: An Anatomical Viewpoint* (Lippincott Williams & Wilkins, Philadelphia), pp 370–371.
34. Toma K, et al. (1999) Activities of the primary and supplementary motor areas increase in preparation and execution of voluntary muscle relaxation: An event-related fMRI study. *J Neurosci* 19:3527–3534.
35. Pandya DN, Vignolo LA (1971) Intra- and interhemispheric projections of the precentral, premotor and arcuate areas in the rhesus monkey. *Brain Res* 26:217–233.
36. Ni Z, et al. (2009) Two phases of interhemispheric inhibition between motor related cortical areas and the primary motor cortex in human. *Cereb Cortex* 19:1654–1665.
37. Byblow WD, et al. (2007) Functional connectivity between secondary and primary motor areas underlying hand-foot coordination. *J Neurophysiol* 98:414–422.
38. Forman SD, et al. (1995) Improved assessment of significant activation in functional magnetic resonance imaging (fMRI): Use of a cluster-size threshold. *Magn Reson Med* 33:636–647.
39. Penfield W, Rasmussen T (1950) *The Cerebral Cortex of Man: A Clinical Study of Localization of Function* (Macmillian, New York), Available at http://www.cengage.com/permissions.